

Lanthanum–molybdenum multilayer mirrors for attosecond pulses between 80 and 130 eV

This article has been downloaded from IOPscience. Please scroll down to see the full text article.

2011 New J. Phys. 13 063038

(<http://iopscience.iop.org/1367-2630/13/6/063038>)

View [the table of contents for this issue](#), or go to the [journal homepage](#) for more

Download details:

IP Address: 130.183.91.154

The article was downloaded on 27/07/2011 at 10:40

Please note that [terms and conditions apply](#).

Lanthanum–molybdenum multilayer mirrors for attosecond pulses between 80 and 130 eV

M Hofstetter^{1,2,6}, A Aquila^{3,4}, M Schultze¹, A Guggenmos^{1,2},
S Yang³, E Gullikson³, M Huth⁵, B Nickel⁵, J Gagnon^{1,2},
V S Yakovlev^{1,2}, E Goulielmakis², F Krausz^{1,2} and
U Kleineberg^{1,2}

¹ Fakultät für Physik, Ludwig-Maximilians-Universität München,
Am Coulombwall 1, 85748 Garching, Germany

² Max-Planck-Institut für Quantenoptik, Hans-Kopfermann-Strasse 1,
85748 Garching, Germany

³ Center for X-Ray Optics, Lawrence Berkeley National Laboratory, 2-400,
1 Cyclotron Road, Berkeley, CA 94720, USA

⁴ Hamburg Center for Free-Electron Laser Science, DESY, Notkestraße 85,
22607 Hamburg, Germany

⁵ Center for NanoScience (CeNS), Ludwig-Maximilians-Universität München,
Schellingstraße 4, 80799 Munich, Germany

E-mail: michael.hofstetter@mpq.mpg.de

New Journal of Physics **13** (2011) 063038 (15pp)

Received 8 March 2011

Published 21 June 2011

Online at <http://www.njp.org/>

doi:10.1088/1367-2630/13/6/063038

Abstract. A novel multilayer material system consisting of lanthanum and molybdenum nano-layers for both broadband and highly reflecting multilayer mirrors in the energy range between 80 and 130 eV is presented. The simulation and design of these multilayers were based on an improved set of optical constants, which were recorded by extreme ultraviolet (XUV)/soft-x-ray absorption measurements on freestanding lanthanum nano-films between 30 eV and 1.3 keV. Lanthanum–molybdenum (La/Mo) multilayer mirrors were produced by ion-beam sputtering and characterized through both x-ray and XUV reflectivity measurements. We demonstrate the ability to precisely simulate and realize aperiodic stacks. Their stability against ambient air conditions is demonstrated. Finally, the La/Mo mirrors were used in the generation of single attosecond pulses from high-harmonic cut-off spectra above 100 eV. Isolated 200 attosecond-long pulses were measured by XUV-pump/IR-probe

⁶ Author to whom any correspondence should be addressed.

streaking experiments and characterized using frequency-resolved optical gating for complete reconstruction of attosecond bursts (FROG/CRAB) analyses.

Contents

1. Introduction	2
2. Experiments and results	3
2.1. Deposition procedure	3
2.2. High-resolution measurement of La optical constants in the extreme ultraviolet (XUV)/soft x-ray range	4
2.3. Simulation of maximum achievable reflectivity	4
2.4. Experimental development and characterization of lanthanum–molybdenum (La/Mo) multilayer mirrors	7
2.5. Aperiodic chirped La/Mo multilayer mirror and long-term stability measurement	8
2.6. Broadband La/Mo mirrors for attosecond pulse generation	11
3. Conclusions	13
Acknowledgment	13
References	13

1. Introduction

Multilayer mirrors allow for (spectrally) tuning extreme ultraviolet (XUV) radiation with very high precision upon reflection. Their reflectivity characteristics can be designed in a flexible manner by a proper choice of the layer materials and the multilayer stack design. First experimental investigations of multilayer optics in the XUV range had already started in the early 1970s [1]; recently, multilayer stacks with complex designs were developed by advanced deposition and design techniques with almost atomically precise interfaces and layer homogeneity [2]. Demanding applications range from EUV lithography [3, 4], soft x-ray microscopy [5] and solar astronomy [6, 7], to hard x-ray monochromators [8].

Recently, multilayer optics were introduced as key elements in the generation of attosecond ($1 \text{ as} = 10^{-18} \text{ s}$) pulses. They are used to filter particular spectral bands from high-harmonic (HH) radiation and give a handle on shaping both the spectral and temporal characteristics of attosecond pulses with a high degree of freedom [9–15]. Such attosecond pulses are intensively used in pump–probe photoelectron spectroscopy to investigate electron and electronic wave-packet dynamics [16–18]. The shortest possible pulse length is inversely proportional to its spectral width, connected via Fourier transform. Therefore, the generation and reflection of ultra-short attosecond pulses depend on the availability of broadband, high-throughput optics for the desired photon energy. The bandwidth ΔE of a periodic multilayer mirror with central energy E can be estimated from the number of contributing periods N : $\Delta E/E \approx 1/N$ [19]. In addition to the spectral filtering properties of such mirrors, the application of them in attosecond physics demands control over the spectral phase. While periodic mirror designs exhibit intrinsically a mostly linear phase, carefully designed aperiodic coatings are required in order to shape the attosecond pulse’s chirp [20, 21]. Furthermore, the stability of the mirrors, against air exposure in particular, and the absence of degradation over time in general are necessary prerequisites for their experimental usage.

Until very recently, energies of broadband HH cut-offs that are appropriate for the generation of isolated attosecond pulses were limited by the available HH sources as well as multilayer optics to photon energies below 100 eV. Nowadays, sources with sufficient photon flux in the HH cut-off between about 30 and about 160 eV exist in various setups [22–26]. We develop mirrors that allow us to extend single attosecond pulse technology to the energy range above 100 eV for the first time. Moving from sub-100 eV photoexcitation energies, where standard Mo–silicon (Mo/Si) coatings can be used, to higher photon energies is of much interest. Attosecond measurements on a larger number of materials become possible, since deeper bound electronic states can be excited by the more energetic photons (such as Si 2p). This could also assist in the generation of ever-shorter attosecond pulses. Attosecond streaking experiments require further the joint presence of both an XUV and a laser pulse. Here, higher XUV photon energies separate the inner-shell photoelectron spectra from unwanted secondary above-threshold-ionization (ATI) electrons to a greater extent and hence give rise to a cleaner photoelectron signal.

So far, high-reflecting multilayer mirrors between 100 and 120 eV have either been based on the toxic element beryllium (Be) with experimental normal incidence reflectivity up to 70% [27–29] or on yttrium (Y) [30] and strontium (Sr) [31] for which a reflectivity of about 45% was achieved. The latter was measured for a 100-bi-layer stack, where the reflectivity measurement was carried out under vacuum conditions due to the high reactivity of Sr to air or water vapor. Standard Mo/Si multilayer mirrors (e.g. [32, 33]) that are used above the Si $L_{2,3}$ –absorption edge suffer both from abrupt changes in the optical constants between about 99 and 115 eV and from the increased absorption of Si, excluding Si-based multilayers as a candidate for attosecond optics in this energy range.

In this paper, we introduce a new multilayer mirror system based on lanthanum (La) and molybdenum (Mo). This material combination is especially suited for broadband optics as required in attosecond physics, as it exhibits high single interface reflectivity in the energy range between 80 and 130 eV. Lanthanum–molybdenum (La/Mo) multilayers exhibit small interface roughness values (σ) of only approximately 0.4 nm. The mirrors are stable against air exposure and consist of nontoxic materials, which cannot be taken for granted in that energy range. This ensures their easy experimental usage. We show that La/Mo multilayer mirrors can be deposited with high accuracy and stability, allowing for the correct realization of periodic and aperiodic stack designs. The combination of La/Mo multilayers with the third material boron carbide (B_4C) adds yet more degrees of freedom for mirror design targets such as high reflectivity, a tailored phase or a special spectral reflectivity shape.

2. Experiments and results

2.1. Deposition procedure

All of the following presented multilayer stacks have been produced by ion-beam deposition (IBD), using (neutralized) 600 eV krypton (Kr) ions. Our deposition system is load-locked. After mounting and pump-down to a base pressure of about 10^{-8} mbar, each target material is cleaned by sputtering for several hours (in the case of lanthanum, typically 20–40 h) to remove any oxides from the sputtering target. Deposition rates of all materials have been smaller than 0.1 nm per second, ensuring good thickness control during the deposition. All three required targets La, Mo and B_4C are mounted on the deposition chamber at the same time. *In-situ* spectral

ellipsometry (an F A Woolam EC 400 ellipsometer together with a Woolam ME2000VI lamp) and profilometry has been used to calibrate the deposition rates of La, Mo and B₄C and control the deposition of each multilayer stack via deposition time.

2.2. High-resolution measurement of La optical constants in the extreme ultraviolet (XUV)/soft x-ray range

In the following, we refer to the established definition of the index of refraction in the XUV as $n = 1 - \delta + i\beta$. The commonly used optical constants of La [34]⁷ lack sufficient spectral accuracy, especially in near-absorption edge features. We measured the optical constants of La between 30 and 1.3 keV using freestanding La foils of different thicknesses (50, 75, 100 and 150 nm) coated with 10 nm B₄C on both surfaces to suppress oxidation. We prepared the foils by depositing each three-layer stack of B₄C/La/B₄C on Si-substrates, which have been coated by a thin film of photoresist (PMMA). The layer thicknesses were obtained from Cu-K_α x-ray reflectivity measurements. Subsequent data analysis revealed e.g. a 49.95 nm-thick La layer between two 9.99 nm-thick B₄C layers on 149.7 nm PMMA and similar good agreement for the other foils. The coated Si wafers were attached to filter supports and the photoresist was dissolved, releasing the thin foil from the Si wafer.

The XUV transmission data of the foils as a function of photon energy were recorded in spectral range between 32 eV and 1.3 keV at beamline 6.3.2 of the Advanced Light Source (ALS) in Berkeley [35]. The real part of the index of refraction δ is calculated from the directly measured absorption part β via the Kramers–Kronig relations [36, 37]. For a more reliable Kramers–Kronig analysis, we added data from other sources to get the full spectrum imaginary part of the index of refraction between 14 eV and 15 keV. Above 1.3 keV, we used data from the *Center for X-Ray Optics* (CXRO) database measured in 2007. Below 32 eV, we completed our dataset with β values from Seely *et al* [38] and Kjornrattanawanich *et al* [39]. After all, we obtained a consistent sum rule value of 55.1 electrons, which is in reasonable agreement with the ideal value of 56.6.

Figures 1(a)–(f) compare our results (blue solid line) with the optical constants that are in common use [34] (depicted by the red dashed line). Due to the improved spectral resolution $\delta E(E_0)$ of the measurements, some deviations from the tabulated data could be revealed. This is most noticeable around 100 eV ($\delta E(100 \text{ eV}) = 0.05 \text{ eV}$) at the $N_{4,5}$ absorption edges (N_4 : 105.3 eV; N_5 : 102.5 eV [40]) (figures 1(a) and (b)) as well as around 840 eV ($\delta E(840 \text{ eV}) = 1 \text{ eV}$) at the $M_{4,5}$ absorption edges (M_4 : 853.0 eV; M_5 : 836.0 eV [40]) (figures 1(e) and (f)). Furthermore, the hardly visible oxygen (O) absorption edge at 543 eV (figures 1(c) and (d)) indicates that the freestanding La films are almost oxygen-free. We thus expect that our La/Mo multilayer mirrors are free from La oxide. These more precise optical constants of La are used in the following for simulations and optimizations of La/Mo multilayer systems.

2.3. Simulation of maximum achievable reflectivity

In the following, we refer to the commonly used terminology to characterize periodic multilayer stacks with bi-layer number N , bi-layer thickness or period d and the ratio of bottom layer thickness to period, γ . Interface imperfections are associated with σ derived as the Névot–Croce [41] parameter $r = r_0 \exp(-2\sigma^2 k_{1s} k_{2s})$, where $k_{1s} = (2\pi/\lambda)n_1 \cos \phi_1$ and $k_{2s} = (2\pi/\lambda)n_2 \cos \phi_2$

⁷ A download link of the latest optical constants can be found at <http://www.cxro.lbl.gov/>

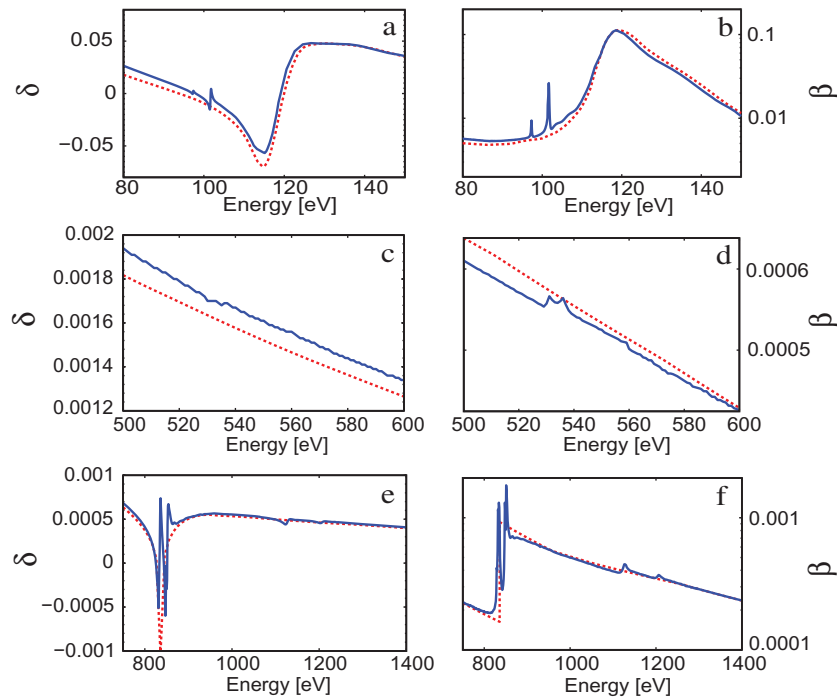


Figure 1. Novel measurement of the optical constants of La. XUV/soft x-ray optical constants (solid blue lines) are displayed in comparison to the commonly used ones from the CXRO database [34] (red dashed curves) for selected energy ranges. The left column displays the δ value, i.e. the deviation of the real part of the refractive index from 1 on a linear scale. The right panels show the imaginary part β of the refractive index on a logarithmic y-scale.

are the perpendicular wave-vector amplitudes and r_0 is the Fresnel reflectivity without roughness. A previous thickness comparison of periodic multilayer and thick single-layer samples revealed an interface contraction of about 0.1 nm per La/Mo and La/B₄C interface and about half of that (0.045 nm) at an Mo/B₄C interface, which indicates inter-diffusion. The Névoť–Croce model describes a single interface reflectivity decrease by continuously varying the optical constants across an interface and does not separate different interface imperfections such as roughness and inter-diffusion, which are mostly indistinguishable in pure reflectivity measurements. We incorporate all imperfection terms in our modeling under σ . The desired layer thicknesses can be successfully implemented by nominally increasing the deposition time of each layer according to the loss. The excellent agreement between the modeled and the measured reflectivity, especially in the case of an aperiodic mirror as presented in figure 5, proves the validity of this approach.

There are in general two extreme cases of periodic multilayer mirror designs: (a) broadband mirrors with high-integrated reflectivity and (b) high reflectivity small-bandwidth coatings. Figure 2 compares the simulated maximum achievable normal incidence peak reflectivity of periodic multilayer stacks built from several material combinations that have been used in the energy range between 80 and 130 eV. Each point in these curves corresponds to a specific multilayer stack, where the thickness of each layer is equal to a quarter of a wavelength ($\gamma = 0.5$). For the La/Mo stack simulation, we assumed an average roughness of 0.4 nm as estimated from experimental data shown later in section 2.4. All other simulations have been

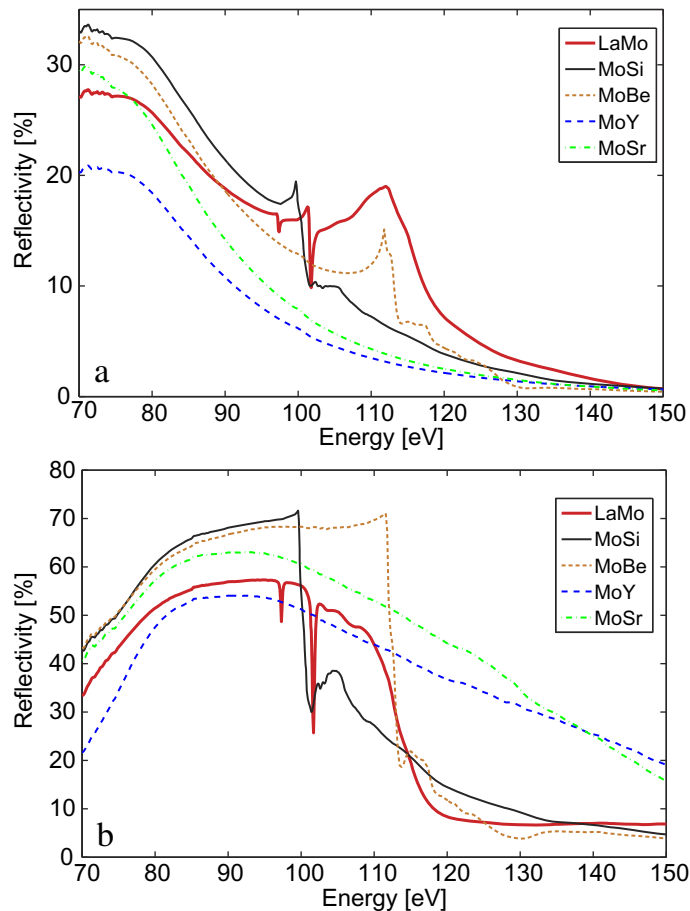


Figure 2. Maximum reflectivity of a quarter-wave stack versus photon energy (simulation): (a) broadband ($N = 8$) and (b) high reflectivity ($N = 100$). Comparison of the maximum achievable peak reflectivity for different material combinations relevant in the energy range between 80 and 150 eV. Each point corresponds to one distinct periodic quarter-wave stack ($\gamma = 0.5$), differing from each other by the bi-layer thickness and the material combination. All simulations were performed with realistic average Nevot–Croce roughness values calculated from existing high-period multilayer mirrors. We use $\sigma = 0.6$ nm for Mo/Si [33] (solid thin black line), $\sigma = 0.55$ nm for Mo/Be [28] (dotted orange line), $\sigma = 0.6$ nm for Mo/Y [29] (dash-dotted blue line) and $\sigma = 0.8$ nm for Mo/Sr [31] (dashed green line). The roughness for our La/Mo stacks (solid thick red) is assumed to be 0.4 nm.

performed with realistic average Névo–Croce parameter values σ of 0.55–0.8 nm retrieved from the literature [27–33].

Figure 2(a) depicts the result from reflectivity simulations for broadband multilayer coatings with eight periods ($\Delta E/E \approx 1/8$). The maximum achievable reflectivity of the few-bi-layer La/Mo multilayer mirrors exceeds that of molybdenum–beryllium (Mo/Be), molybdenum–strontium (Mo/Sr) or molybdenum–yttrium (Mo/Y). This changes when we look at the case of high-periodic multilayer mirrors (figure 2(b)). This simulation was performed for

100-period, optically thick stacks to ensure saturated maximum reflectivity R_∞ of all material combinations. Around 110 eV the maximum achievable reflectivity of a La/Mo multilayer is about 25% lower than that of a Mo/Be stack in the large period case. La and Mo exhibit a larger Fresnel reflectivity and a lower roughness than e.g. Mo and Be. On the other hand, the XUV absorption in La is also larger, leading to a lower penetration depth. At 110 eV La/Mo multilayers reveal reflectivity saturation (95% of R_∞) for only 25 periods, while many more bi-layers may contribute to the simulated maximum reflectivity for other material combinations (e.g. more than 43 periods for Mo/Be). That is why the La/Mo eight-bi-layer stack outperforms the other material combinations, while it is not exhibiting the highest reflectivity for the 100-bi-layer stack.

In ultrafast physics, broadband mirrors are required that preserve the pulse length. Broadband reflective coatings could as well be produced with large-period aperiodic stacks that contain low-absorption materials [42, 43], but here the nonlinear spectral phase would yield a temporal broadening of a Fourier-limited pulse after reflection. This becomes obvious when estimating the number of periods of a multilayer coating for attosecond pulse reflection from the following simple geometrical argument. It relates the pulse duration τ directly to the stack height h : pulse components that are reflected at the top of the mirror must temporally interfere with pulse components being reflected at the bottom: $2h \approx c\tau$ where c is the speed of light. For a $\tau = 200$ as long pulse, this yields a height of about 30–50 nm. Thus no more than ten bi-layer periods (1 period is approximately $\lambda/2 \approx 5$ nm) may contribute.

In conclusion, the combination of La and Mo is the favorable choice for high-throughput broadband multilayer optics for the generation of nearly transform-limited attosecond pulse from the chirp-free HH cut-off spectrum between 80 and 130 eV.

2.4. Experimental development and characterization of lanthanum–molybdenum (La/Mo) multilayer mirrors

In this section, experimental results on high-period La/Mo stacks are presented. We have carried out x-ray reflectometry (XRR) measurements for a 36-period Mo/La stack capped with 3 nm B_4C to suppress oxidation. A Mo- K_α x-ray source at 17.4 keV ($= 0.07$ nm) was used. Figure 3 shows the result of this measurement (green curve) together with a simulation (black dashed line). The simulation reveals a bi-layer thickness d of 5.72 nm and $\gamma = 0.47$ in good agreement with the designed $d = 5.72$ nm and $\gamma = 0.45$. The Névo–Croce roughness could be estimated to be 0.3 nm. Both the finite source angle and the detector acceptance angle have been taken into account in the simulation. This mirror is assigned as mirror ‘A’ in the following.

Figure 4 shows the result of XUV measurements for four different high-reflectivity La/Mo mirrors centered at different photon energies (colored curves), performed again at the CXRO beamline 6.3.2 at the ALS under an angle of 5° off-normal incidence, together with corresponding reflectivity simulations (black dashed lines). We have produced La/Mo multilayer stacks with and without passivating B_4C interface layers between the materials La and Mo. The small inset in figure 4 compares mirror A with an identical multilayer stack D (the same d , γ and N) that contains small 1 nm B_4C interlayers. The XUV reflectivity hardly changes; therefore, we often work with thin (1 nm or less) passivating B_4C interlayers in our stacks as we expect higher stability.

We find nearly perfect agreement between the measurement and the simulations using the new optical constants of La. The XUV measurements further confirm the very low average

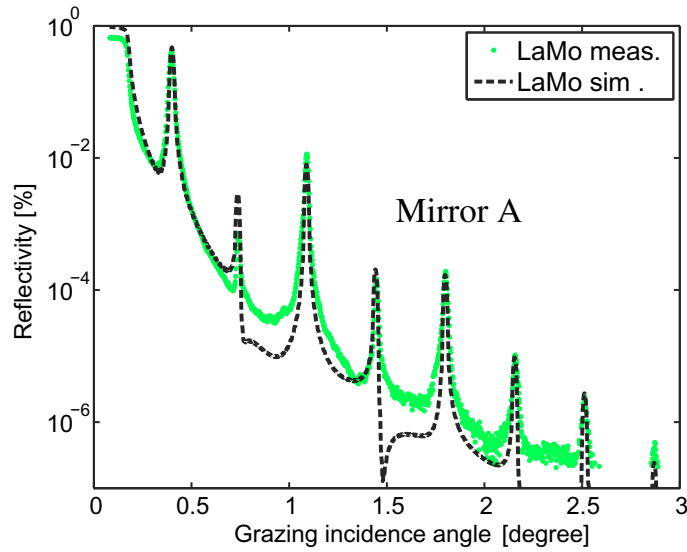


Figure 3. XRR measurement and simulation. Comparison of a small-angle x-ray reflectivity measurement (green line) at Mo- K_{α} ($\lambda = 0.07$ nm) and its corresponding fit simulation (black dashed line) for a high-reflectivity 36-bi-layer Mo/La mirror ($d = 5.72$ nm, $\gamma = 0.47$, $\sigma = 0.3$ nm; 3 nm B₄C capping layer). This mirror is referred to as mirror A in the following.

roughness. We deduce an XUV roughness of only 0.4 nm in the case of pure La/Mo multilayer stacks and about 0.6 nm when the mirrors contain B₄C barrier layers. This value appears slightly higher than the 0.3 nm that was extracted from XRR simulations (figure 3). This deviation could originate from the different penetration depths in both measurements.

The remarkable agreement between the XUV measurement of mirror A and the simulation performed with parameters extracted from the XRR fit (figure 3) indicates a correct characterization of the system. We measure large near-normal incidence peak reflectance as simulated in figure 2(b). For mirror A we find 41.5% at 109 eV and 31.5% at 112 eV for the 20-bi-layer ($R \approx 90\% R_{\infty}$) mirror C. For stacks centered at slightly lower photon energies, an even higher reflectivity of more than 44% (mirror B at 105 eV) has been measured and supported by corresponding simulations (see figure 2(b)).

2.5. Aperiodic chirped La/Mo multilayer mirror and long-term stability measurement

Chirp control is an essential task when shaping attosecond pulses, especially if one wants to generate Fourier-limited attosecond pulse trains from the HH plateau region, which is well known to carry chirp [43]. We have developed and produced aperiodic La/Mo stacks at ≈ 105 eV, which introduce/compensate group delay dispersion ($GDD = -d^2\phi/d\omega^2$) of more than $\pm 10\,000$ as² per single reflection. The useful bandwidth of those mirrors supports a Fourier-limited pulse duration of 200 as and the mirrors reveal a high reflectivity of about 10% under normal incidence. These aperiodic stacks have been designed using evolutionary algorithms [44]. We include B₄C as an additional material in our designs. This gives us a larger parameter space to explore in our multiple design goals, namely a broad bandwidth, an essential

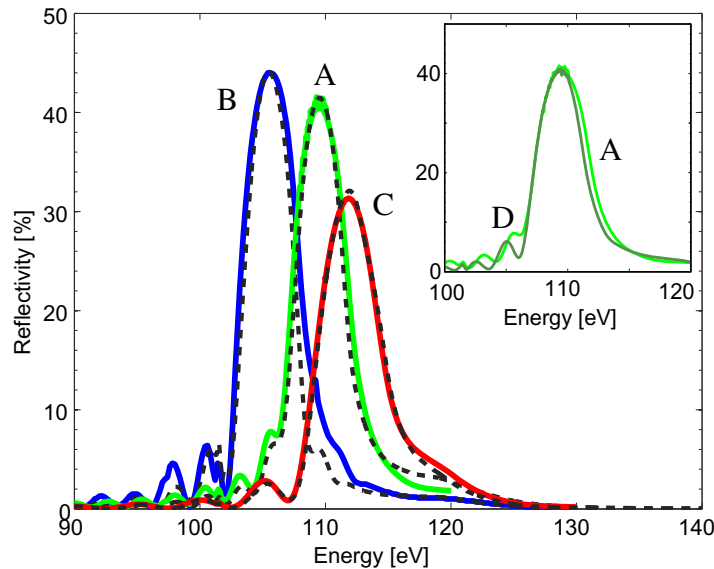


Figure 4. XUV reflectivity measurement of different high-reflectivity La/Mo stacks. XUV measurements (solid colored lines) of different high-periodic La/Mo mirrors, together with their simulated reflectivity (black dotted lines). Mirror A (light green) is the 36-period ($R > 99\%R_\infty$) stack characterized by XRR in figure 3 (see the caption of figure 3 for design details), mirror B (blue) is a 30-period ($R > 99\%R_\infty$) Mo/La mirror stack with $\gamma = 0.55$ centered at 105 eV (capping 5 nm). Mirror C (red) has 20 bi-layers ($R \approx 90\%R_\infty$), a period of 5.61 nm and $\gamma = 0.55$ and contains 0.6 nm B_4C inter-diffusion layers and a 3 nm B_4C capping layer. The small inset compares XUV reflectivity measurements of mirror A with an equivalent mirror D that contains 1 nm B_4C barrier layers.

amount of GDD, a large peak reflectivity and a low reflectivity outside the useful spectral range. Furthermore, B_4C is used as a passivating interlayer between Mo and La and as a capping layer on top of the stack.

Figure 5 exemplarily shows the simulated (black line) and the measured (blue curves) reflectivity, as well as the simulated phase (red dashed lines) of a mirror, which adds a GDD of $-10\,000\text{ as}^2$ to the incoming pulse. This mirror has been designed to be used in combination with a thin (about 200 nm-thick) palladium (Pd) foil, which suppresses photons below 95 eV for a spectrally and temporally clean attosecond pulse. The aperiodic design contains La layer thicknesses between 1.6 and 16 nm, Mo layers between 2.1 and 4.8 nm and B_4C layer thicknesses between 1 and 10 nm (figure 5(b)). A Fourier-limited Gaussian pulse of 200 as (FWHM) would be stretched to more than 300 as by one reflection. This design exhibits an extreme case of almost maximum possible chirp for a given bandwidth. Designs with less GDD (of both signs) or less bandwidth would be easy to implement.

La is a highly reactive material and tends to oxidize within a short amount of time. To examine the degradation of the multilayer reflectivity over time, especially when stored in ambient air conditions, we have measured the long-term reflectivity stability of this mirror. After deposition, the samples were sealed water-free under nitrogen environment and then

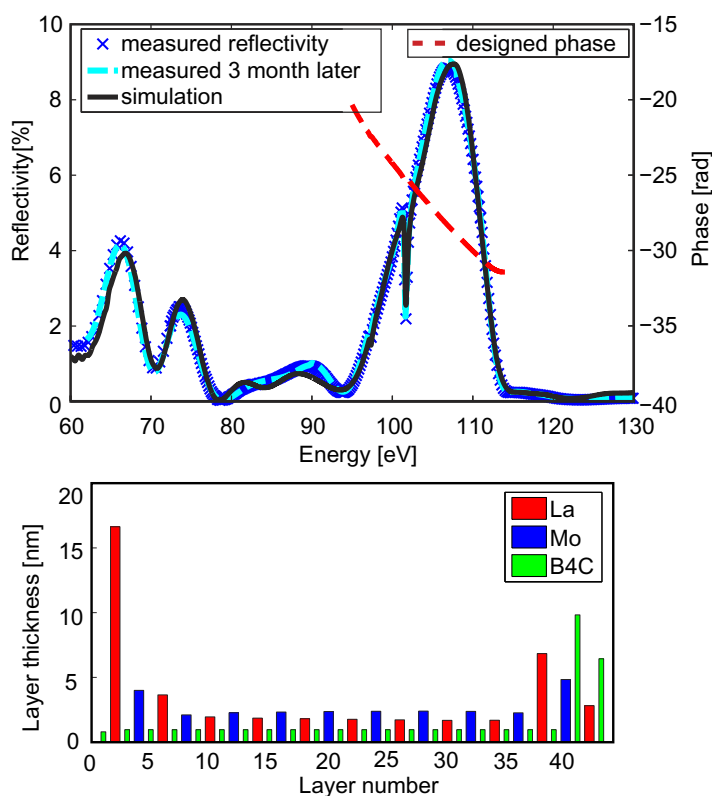


Figure 5. Shelf lifetime test of an aperiodic chirped mirror. Simulated reflectivity (black solid line) and phase (red dashed line) together with the measured XUV reflectivity (blue/cyan plots) for an aperiodic La/Mo/B₄C stack. The blue crosses depict the result of the XUV measurement right after sealing in nitrogen environment, while the dashed cyan line shows the outcome of a measurement of the same sample after air exposure over 3 months. The lower panel shows the appropriate aperiodic design.

brought into the reflectivity measurement chamber, keeping transition times as short as possible. A second measurement was carried out 3 months later after storing the same sample under ambient humidity, pressures and room temperature between measurements. This mirror has not been irradiated by XUV/x-ray light, except for the two reflectivity measurements.

Aperiodic mirrors are very suitable for testing the stability of a material combination, as they are more likely to exhibit slight variations due to the very different layer thicknesses and therefore less-stable designs (e.g. aperiodic multilayers are more sensitive to layer compression, layer expansion, and inner layer phase transitions [45]). Figure 5 shows excellent agreement between both measurements with the designed reflectivity. The average Névoť–Croce roughness could be estimated to be about 0.55 nm, in very good agreement with the earlier performed high-period sample fits from figures 3 and 4.

In conclusion, we find that this material combination allows for a broad tunability in the design of mirrors above 100 eV; it is easy to handle during fabrication and enables the stable production of also aperiodic mirrors.

2.6. Broadband La/Mo mirrors for attosecond pulse generation

We have designed and produced a La/Mo-coated ‘double mirror’ for the generation of isolated attosecond pulses and characterized those via electron streaking [46] in neon. We demonstrated the pulse shaping abilities of our mirror at the AS1 beamline of the Max Planck Institute of Quantum Optics (MPQ) in Garching. The experiment has been performed in the typical collinear XUV-pump/IR probe scheme described e.g. in [12]. Single attosecond pulse generation requires HH radiation generated from a few-cycle phase-stabilized femtosecond ($1 \text{ fs} = 10^{-15} \text{ s}$) laser pulses [47–49]. The mirror is used to spectrally isolate a single attosecond pulse from the high-energy cut-off part of that coherent HH XUV radiation.

The aim of this particular experiment was to generate nearly Fourier-limited 200 as pulses with a central energy of about 109 eV in the cut-off part of the HH generation spectrum in neon gas. We used this mirror to probe the dynamics of photoionization of the s and p subshells in neon [18]. Figure 6 concludes the results of our mirror design and the experiment. The mirror was designed for combined use with a 150 nm Pd filter, which suppresses the low-energy spectral components (as depicted by the yellow curve in figure 6(a)). Additional high-energy suppression above 130 eV via the intrinsic drop in photon flux from the HH cut-off of our source was taken into account in the design (figure 6(a), gray line). We chose a periodic La/Mo design with $N = 8$, $\gamma = 0.47$, $d = 6.05 \text{ nm}$ as being appropriate for our requirements. B_4C interlayers as well as a B_4C capping layer have been included in the design.

The final design exhibits a maximum reflectivity of about 15% centered at 107 eV and reflects over a bandwidth of about 11 eV, as depicted by the solid black line in figure 6(a). The dashed black line depicts the expected XUV spectrum as the multiplication of an artificial Gaussian HH spectrum and the transmission of the Pd filter and exhibits maximum intensity at 108.8 eV. Comparing this simulation with the measured photoelectron spectrum (green dotted line in figure 6(a)) in the absence of the laser field (shifted by the binding energy in neon of 21.6 eV), we found reasonable agreement.

The question arises whether the La $N_{4,5}$ absorption edges around 100 eV visible in figures 1(a) and (b) and 6(a) affect the temporal shape of the reflected attosecond pulses. We have simulated the temporal structure of the pulse from its convolution of the HH cut-off radiation (which is assumed to be chirp free), the filter and the mirror. Depending on the shape of the HH cut-off, we expect Fourier-limited pulses with durations between 190 and 210 as and a bandwidth of about 10 eV. Moreover, we find that the spectral phase extends the pulse duration to not more than 10 as beyond its Fourier limit. This includes the effects on the pulse due to phase discontinuities around 100 eV and the Pd filter. The reason why this broadening appears to be so little is the sharpness of $N_{4,5}$ absorption lines; each of them is confined to a spectral range of sub-1 eV only. Thus, the total amount of power spread out to large time values is actually quite small.

To characterize our attosecond pulses experimentally, we used the typical XUV pump/IR probe streaking technique [12, 50]. Here, both the attosecond XUV pulse and the IR laser pulse are focused into neon gas. The XUV pulse generates photoelectrons, which are streaked by the co-propagating temporally synchronized and phase stable IR laser electric field. The inner part of the double mirror can be moved with respect to the outer part, allowing us to introduce a temporal delay between the XUV pulse, which is reflected at the mirror core, and the laser pulse, which is reflected at the outer ring. Changing the delay between the laser and

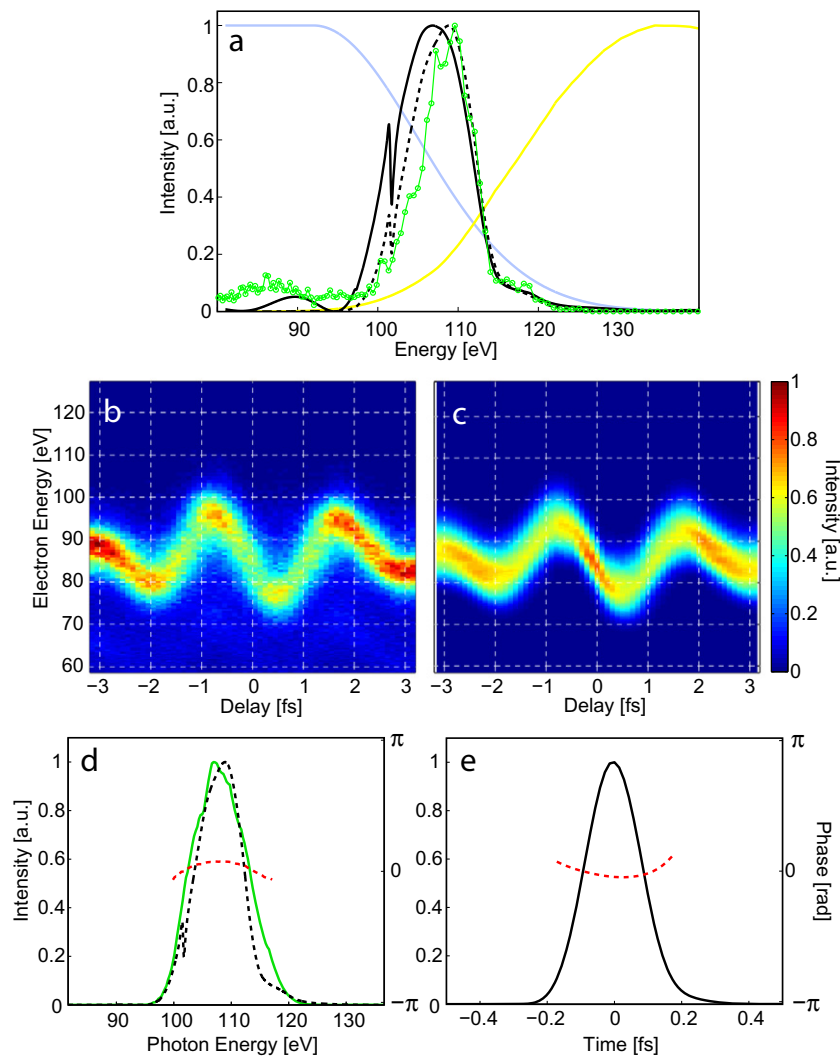


Figure 6. Broadband La/Mo mirror for attosecond pulse generation. (a) Comparison of the photoelectron spectrum measured without the streaking field (green dotted line) and the expected XUV spectrum (black dashed line). The latter spectrum was calculated from the simulated mirror reflectivity (solid black line), the filter transmission (yellow curve) and an artificial HH spectrum (light blue curve). (b–e) Results of a streaking experiment performed with the mirror shown in (a). The middle panels compare the measured (b) and the retrieved (c) electronic streaking trace performed via FROG/CRAB analyses. The lower panels show the retrieved XUV pulse (green and black solid lines) and the retrieved phase (red dashed line) in the spectral (d) and the temporal (e) domain. The mirror reflectivity multiplied by the transmission of the Pd filter is additionally plotted in figure 6(d) (black dashed line).

the XUV attosecond pulse yields a typical streaking spectrogram (figure 6(b)). The absence of interference fringes and the presence of only one streaking curve in our spectrogram reveal clearly that there is only a single, isolated attosecond pulse exiting the mirror, which further confirms our expectations of only minor phase effects.

FROG/CRAB [51] analysis allows for a complete reconstruction of both the intensity and the chirp of the XUV attosecond pulse as well as the vector potential of the streaking laser field from a recorded spectrogram (figure 6(b)). Figure 6(c) shows the result of the appropriate FROG/CRAB retrieval as described by Gagnon and coworkers in [52, 53]. Figures 6(d) and 6(e) display the retrieved intensity (green line) and phase (red dashed line) of the XUV pulse, once in the spectral and once in the temporal domain. The expected XUV spectrum (black dashed line in figure 6(a)) is additionally plotted in figure 6(d) for comparison. With the retrieved spectral bandwidth and phase, being the most prominent sources of uncertainty, the error can be estimated to be about 10 as. We find an attosecond pulse of about 200 as, in excellent agreement with our previous estimations.

3. Conclusions

We have applied a novel multilayer material combination La/Mo for the generation of isolated attosecond pulses at photon energies just above 100 eV. Proper simulations of the reflectivity and the phase of multilayer mirrors could only be performed after measuring the soft x-ray optical constants of La with a high spectral resolution. We have assessed the long-term stability of an aperiodic mirror in ambient air by XUV reflectometry measurements and we observed no measurable degradation. Aperiodic multilayer mirrors have been introduced and give a promising outlook on tailor-made La/Mo mirrors. In particular, their high reflectance at each interface allows the design of broadband mirrors with a large integrated reflectivity. We have investigated the effect of La absorption edges around 100 eV on the pulse length, both theoretically and experimentally, and found that these edges hardly influence the filtered attosecond pulse. Thus, La/Mo coatings are key to the generation of isolated attosecond pulses with central energies around 105 eV, just as Mo/Si mirrors are suitable below 100 eV.

Acknowledgment

This work was supported by the DFG Excellence Cluster ‘Munich Centre for Advanced Photonics’ (MAP).

References

- [1] Spiller E 1972 Low-loss reflection coatings using absorbing materials *Appl. Phys. Lett.* **20** 365
- [2] Erikson F, Ghafoor N, Schäfers F, Gullikson E M, Aouadi S, Rohde S, Hultman L and Birch J 2008 Atomic scale interface engineering by modulated ion-assisted deposition applied to soft x-ray multilayer optics *Appl. Opt.* **47** 23
- [3] Gwyn C W, Stulen R, Sweeney D and Attwood D 1998 Extreme ultraviolet lithography *J. Vac. Sci. Technol. B* **16** 3142
- [4] Wagner C and Harned N 2010 EUV lithography: lithography gets extreme *Nat. Photonics* **4** 24–6
- [5] Chao W, Harteneck B D, Liddle J A, Anderson E H and Attwood D T 2005 Soft X-ray microscopy at a spatial resolution better than 15 nm *Nature* **435** 1210–3
- [6] Martinez-Galarce D S, Walker A B, Gore D B, Kankelborg C C, Hoover R B, Barbee T W and Boerner P F 2000 High resolution imaging with multilayer telescopes: resolution performance of the MSSTA II Telescopes *Opt. Eng.* **39** 1063–79
- [7] Schäfers F *et al* 1999 Soft-X-ray polarimeter with multilayer optics: Complete analysis of the polarization state of light *Appl. Opt.* **38** 4074–88

- [8] André J M *et al* 2002 X-ray multilayer monochromator with enhanced performance *Appl. Opt.* **41** 239–44
- [9] Wonisch A, Westerwalbesloh T, Hachmann W, Kabachnik N, Kleineberg U and Heinzmann U 2004 Aperiodic nanometer multilayer systems as optical key components for attosecond electron spectroscopy *Thin Solid Films* **464–465** 473–7
- [10] Wonisch A, Neuhäusler U, Kabachnik N M, Uphues T, Uiberacker M, Yakovlev V, Krausz F, Drescher M, Kleineberg U and Heinzmann U 2006 Design, fabrication, and analysis of chirped multilayer mirrors for reflection of extreme-ultraviolet attosecond pulses *Appl. Opt.* **45** 4147–56
- [11] Morlens A S, Laude V, Kasamias S, Balcou P, Zeitoun P and Valentin C 2005 Compression of attosecond harmonic pulses by extreme-ultraviolet chirped mirrors *Opt. Lett.* **30** 1554–6
- [12] Schultze M, Goulielmakis E, Uiberacker M, Hofstetter M, Kim J, Kim D, Krausz F and Kleineberg U 2007 Powerful 170-attosecond XUV pulses generated with few-cycle laser pulses and broadband multilayer optics *New J. Phys.* **9** 243
- [13] Goulielmakis E *et al* 2008 Single-cycle nonlinear optics *Science* **320** 1614–7
- [14] Suman M, Monaco G, Pelizzo M G, Windt D L and Nicolosi N 2009 Realization and characterization of an XUV multilayer coating for attosecond pulses *Opt. Express* **17** 7922–32
- [15] Hofstetter M *et al* 2010 First attosecond pulse control by multilayer mirrors above 100 eV photon energy *Proc. Int. Conf. on Ultrafast Phenomena XVII, 11.17* ed M Chergui, D Jonas, E Riedle, B Schönlein and A Taylor (New York: Oxford University Press) <http://www.opticsinfobase.org/abstract.cfm?uri=UP-2010-PDP8>
- [16] Cavalieri A L *et al* 2007 Attosecond spectroscopy in condensed matter *Nature* **449** 1029–32
- [17] Uiberacker M *et al* 2007 Attosecond real-time observation of electron tunneling in atoms *Nature* **446** 627–32
- [18] Schultze M *et al* 2010 Delay in photoemission *Science* **328** 1658
- [19] Spiller E 1994 *Soft X-Ray Optics* (Bellingham, WA: SPIE Optical Engineering Press)
- [20] Aquila A, Salmassi F and Gullikson E 2008 Metrologies for the phase characterization of attosecond extreme ultraviolet optics *Opt. Lett.* **33** 455–7
- [21] Hofstetter M *et al* 2011 Attosecond dispersion control by extreme ultraviolet multilayer mirrors *Opt. Express* **19** 3
- [22] Sansone G *et al* 2006 Isolated single-cycle attosecond pulses *Science* **314** 5798
- [23] Kim S, Jin J, Kim Y J, Park Y J, Kim Y and Kim S W 2008 High-harmonic generation by resonant plasmon field enhancement *Nature* **453** 757–60
- [24] Pfeifer T, Abel M J, Nagel P M, Boutu W, Bell M J, Liu Y, Neumark D M and Leone S R 2009 Measurement and optimization of isolated attosecond pulse contrast *Opt. Lett.* **34** 1819–21
- [25] Fieß M, Schultze M, Goulielmakis E, Dennhardt B, Gagnon J, Hofstetter M, Kienberger R and Krausz F 2010 Versatile apparatus for attosecond metrology and spectroscopy *Rev. Sci. Instrum.* **81** 093103
- [26] Magerl E *et al* 2011 A flexible apparatus for attosecond photoelectron spectroscopy of solids and surfaces *Rev. Sci. Instrum.* **82** 063104
- [27] Skulina K M, Alford C S, Bionta R B, Makowiecki D M, Gullikson E M, Soufli R, Kortright J B and Underwood J H 1995 Molybdenum/beryllium multilayer mirrors for normal incidence in the extreme ultraviolet *Appl. Opt.* **34** 3727
- [28] Montcalm C, Bajt S, Mirkarimi P, Spiller E, Weber F and Folta J 1998 Multilayer reflective coatings for extreme-ultraviolet lithography *Proc. SPIE* **3331** 42
- [29] Bajt S *et al* 2000 Molybdenum–ruthenium/beryllium multilayer coatings *J. Vac. Sci. Technol. A* **18** 557–9
- [30] Montcalm C, Sullivan B T, Duguay S, Ranger M, Steffens W, Pépin H and Chaker M 1995 *In situ* reflectance measurements of soft-x-ray/extreme-ultraviolet Mo/Y multilayer mirrors *Opt. Lett.* **20** 1450–2
- [31] Sae Lao and Montcalm C 2001 Molybdenum–strontium multilayer mirrors for the 8–12-nm extreme-ultraviolet wavelength region *Opt. Lett.* **26** 468–70
- [32] Barbee T W, Mrowka S and Hettrick M C 1985 Molybdenum-silicon multilayer mirrors for the extreme ultraviolet *Appl. Opt.* **24** 883–6
- [33] Bajt S, Alameda J, Barbee Jr T, Clift W M, Folta J A, Kaufmann B and Spiller E A 2002 Improved reflectance and stability of Mo-Si multilayers *Opt. Eng.* **41** 1797–804

- [34] Henke B L, Gullikson E M and Davis J C 1993 X-ray interactions: photoabsorption, scattering, transmission, and reflection at $E = 50\text{--}30\,000\text{ eV}$, $Z = 1\text{--}92$ *At. Data Nucl. Data Tables* **54** 181–342
- [35] Underwood J H and Gullikson E M 1992 High-resolution, high-flux, user friendly VLS beamline at the ALS for the 50–1300 eV energy region *J. Electron. Spectrosc. Relat. Phenom.* **92** 265–72
- [36] Kronig R. and de L 1926 On the theory of the dispersion of x-rays *J. Opt. Soc. Am.* **12** 547–57
- [37] Kramers H A 1927 La diffusion de la lumiere par les atomes *Atti Cong. Intern. Fisica (Trans. Volta Cent. Congr.) (Como, Italy)* vol 2, pp 545–57
- [38] Seely J F, Uspenskii Y A, Kjornrattanawanich B and Windt D L 2006 Coated photodiode technique for the determination of the optical constants of reactive elements: La and Tb *SPIE Proc.* **6317** 63170T
- [39] Kjornrattanawanich B, Windt D L, Bellotti J A and Seely J F 2009 Measurement of dysprosium optical constants in the 2–830 eV spectral range using a transmittance method, and compilation of the revised optical constants of lanthanum, terbium, neodymium, and gadolinium *Appl. Opt.* **48** 3084–93
- [40] Cardona M and Ley L 1978 *Photoemission in Solids. General Principles* (Berlin: Springer)
- [41] Névot L and Croce P 1980 Caractérisation des surfaces par réflexion rasante de rayons X. Application à l'étude du polissage de quelques verres silicates *Rev. Phys. Appl.* **15** 761–79
- [42] Ménesguen Y, de Rossi S, Meltchakov E and Delmotte F 2009 Aperiodic multilayer mirrors for efficient broadband reflection in the extreme ultraviolet *Appl. Phys. A* **98** 305–9
- [43] Mairesse Y *et al* 2003 Attosecond synchronization of high-harmonic soft X-rays *Science* **302** 1540–3
- [44] Tikhonravov A V, Trubetskov M K and DeBell G W 2007 Optical coating design approaches based on the needle optimization technique *Appl. Opt.* **46** 704–10
- [45] Aquila A L, Salmassi F, Dollar F, Liu Y and Gullikson E 2006 Developments in realistic design for aperiodic Mo/Si multilayer mirrors *Opt. Express* **14** 10073–8
- [46] Kienberger R *et al* 2002 Steering attosecond electron wave packets with light *Science* **297** 1144–8
- [47] Cavalieri A L *et al* 2007 Intense 1.5-cycle near infrared laser waveforms and their use for the generation of ultra-broadband soft-x-ray harmonic continua *New J. Phys.* **9** 242
- [48] Kitzler M, Milosevic N, Scrinzi A, Krausz F and Brabec T 2002 Quantum theory of attosecond XUV pulse measurement by laser dressed photoionization. *Phys. Rev. Lett.* **88** 173904
- [49] Krausz F and Ivanov M 2009 Attosecond physics *Rev. Mod. Phys.* **81** 163–234
- [50] Kienberger R *et al* 2004 Atomic transient recorder. *Nature* **427** 817–21
- [51] Trebino R *et al* 1997 Measuring ultrashort laser pulses in the time-frequency domain using frequency-resolved optical gating *Rev. Sci. Instrum.* **68** 3277
- [52] Gagnon J and Yakovlev V S 2009 The robustness of attosecond streaking measurements *Opt. Express* **17** 17678–93 <http://www.attoworld.de/Home/ourResearch/Downloads/index.html>
- [53] Gagnon J, Goulielmakis E and Yakovlev V S 2008 The accurate FROG characterization of attosecond pulses from streaking measurements *Appl. Phys. B* **92** 25–32